Biochimica et Biophysica Acta – Biomembranes 1859 (2017) 813-823

The voltage-sensitive dye RH421 detects a Na^+,K^+-ATPase conformational change at the membrane surface

Alvaro Garcia[a], Promod R. Pratap[b], Christian Lüpfert[c], Flemming Cornelius[d], Denis Jacquemin[e,f], Bogdan Lev[g], Toby W. Allen[g,h], and Ronald J. Clarke[a,*]

[a] *School of Chemistry, University of Sydney, Sydney, NSW 2006, Australia*

[b] *Department of Physics and Astronomy, University of North Carolina at Greensboro, Greensboro NC 27402-6170, U.S.A.*

[c] *Department of Biophysical Chemistry, Max-Planck-Institute of Biophysics, D-60438 Frankfurt am Main, Germany*

[d] *Department of Biomedicine, University of Aarhus, DK-8000 Aarhus C, Denmark*

[e] *CEISAM Lab, UMR CNRS 6230, Science and Technology Faculty, BP92208, University of Nantes, 44322 Nantes Cedex 3, France*

[f] *Institut Universitaire de France, 1, Rue Descartes, 75231-Paris, France*

[g] *School of Applied Science and Health Innovations Research Institute, RMIT University, Melbourne, Australia*

[h] *Department of Chemistry, University of California, Davis, CA 95616, USA*

Address correspondence to Assoc. Prof. Ronald J. Clarke, School of Chemistry, University of Sydney, Sydney, NSW 2006, Australia. Tel.: 61-2-93514406; Fax: 61-2-93513329; E-mail: ronald.clarke@sydney.edu.au.

Abstract

RH421 is a voltage-sensitive fluorescent styrylpyridinium dye which has often been used to probe the kinetics of Na^+,K^+-ATPase partial reactions. The origin of the dye's response has up to now been unclear. Here we show that RH421 responds to phosphorylation of the Na^+,K^+-ATPase by inorganic phosphate with a fluorescence increase. Analysis of the kinetics of the fluorescence response indicates that the probe is not detecting phosphorylation itself but rather a shift in the protein's E1/E2 conformational equilibrium induced by preferential phosphate binding to and phosphorylation of enzyme in the E2 conformation. Molecular dynamics simulations of crystal structures in lipid bilayers indicate some change in the protein's hydrophobic thickness during the E1-E2 transition, which may influence the dye response. However, the transition is known to involve significant rearrangement of the protein's highly charged lysine-rich cytoplasmic N-terminal sequence. Using poly-L-lysine as a model of the N-terminus, we show that an analogous response of RH421 to the E1 → E2P conformational change is produced by poly-L-lysine binding to the surface of the Na^+,K^+-ATPase-containing membrane fragments. Thus, it seems that the prime origin of the RH421 fluorescence response is a change in the interaction of the protein's N-terminus with the surrounding membrane. Quantum mechanical calculations of the dye's visible absorption spectrum give further support to this conclusion. The results obtained indicate that membrane binding and release of the N-terminus of the Na^+,K^+-ATPase α-subunit are intimately involved in the protein's catalytic cycle and could represent an effective site of regulation.

Keywords: RH421 fluorescence; Na^+,K^+-ATPase; stopped-flow kinetics; molecular dynamics; N-terminus; phosphorylation

1. Introduction

Voltage-sensitive or electric field sensitive membrane probes were first introduced in the 1970s and have since undergone a long development to improve sensitivity, time resolution and photochemical stability [1-10]. One of their earliest applications was in the optical detection of action potentials of neurons, for which they continue to be used. For this application a fast response to changes in intramembrane electric field is essential. Response times in the sub-nanosecond time range can in principle be achieved by dyes whose absorbance or fluorescence response is based on an electric-field-induced redistribution of the dye's electron cloud, i.e. via an electrochromic mechanism [11, 12]. This was realised by Loew and collaborators [13], who, based on extended-Hückel calculations, first proposed the aminostyrylpryridinium chromophore as a potential candidate for the development of effective electrochromic dyes. Such dyes have since been widely used for the imaging of electrical events in cells, cell organelles, vesicles and even in a living brain [3, 5-7, 14]. Examples of these dyes include those generally known simply by their abbreviations RH, ANEPPS and ANNINE.

In 1988 it was shown by Klodos and Forbush [15] that the dye RH160 responded to the activity of an ion pump, the Na^+,K^+-ATPase, in open membrane fragments. Because the membrane fragments were open and completely surrounded by aqueous solution on all sides no transmembrane potential could be present. The dye must have been responding to an intramembrane electric field strength change or by interacting directly with the protein. Since then such dyes, but particularly RH421, have been extensively used to resolve the kinetics of ion pumps and to obtain information on their mechanisms [16-24]. However, the question remains as to what the dyes are actually detecting. It has been suggested that the dyes detect electric field strength changes arising from the binding of transported ions to binding sites within the protein [19, 25]. This would seem to be a logical explanation, because it is known

from electrophysiological studies that the kinetics of ion binding steps of the Na^+,K^+-ATPase are dependent on the transmembrane potential [26-30], indicating that the ion binding steps are electrogenic. However, the electrogenic binding of ions are coupled to protein conformational changes which occlude the ions within the protein matrix. This makes it exceedingly difficult to conclusively determine whether the origin of the RH421 response is actually due to ion binding itself or to the associated occlusion reaction. In fact, recent results have cast doubt on the validity of ion binding as an explanation for the dye's fluorescence responses.

Electric field strength calculations [31] based on recent X-ray crystal structures of the Na^+,K^+-ATPase have shown that the electric fields produced by Na^+ and K^+ ions binding to the protein are expected to be effectively screened by the protein matrix before one reaches the location of the dye at the membrane-aqueous solution interface adjacent to the protein. Furthermore, it was shown that the benzyltriethylammonium ion (BTEA), which is known to bind in a voltage-dependent fashion to the Na^+,K^+-ATPase but not undergo occlusion within the protein [32-34], did not produce the fluorescence change expected if ion binding alone were responsible for the dye's response [31]. Grădinaru and Apell [25], on the other hand, suggested that BTEA may not cause a fluorescence drop because it is too bulky to penetrate all the way to the K^+ binding sites of the protein and may bind in a non-electrogenic fashion within a relatively shallow water-filled cavity. They conceded, however, that they couldn't reconcile this hypothesis with the experimental results of Peluffo et al. [33] showing voltage-dependent BTEA binding. The attribution of the RH421 fluorescence changes to protein conformational changes [31, 35-37] would gain considerable support if the presence of a fluorescence change could be demonstrated from a pure conformational change of a protein in the complete absence of any ion binding to the protein's ion transport sites. That is what we will show here.

The Na^+,K^+-ATPase exists in two major conformations, which can be in phosphorylated or nonphosphorylated states, termed E1(P) and E2(P). The nonphosphorylated E1 state is stabilized by Na^+ ions, whereas the nonphosphorylated E2 state is stabilized by K^+ ions. Under normal physiological conditions, enzyme in the E1 state with bound Na^+ ions becomes phosphorylated by ATP and then undergoes a relaxation to the E2P state. Extracellular K^+ ions then stimulate a rapid dephosphorylation of the protein. However, in the complete absence of both Na^+ and K^+ it is possible to phosphorylate the protein by inorganic phosphate, P_i. This reaction occurs via P_i reacting with enzyme in the E2 state. This is the reverse of the physiological dephosphorylation reaction. For this reason it is often referred to as "back-door" phosphorylation. Because the E2 conformation of the protein is preferentially phosphorylated over the E1 conformation, back-door phosphorylation perturbs the protein's E1/E2 conformational equilibrium in favour of E2 [38, 39]. Therefore, it is an ideal reaction to investigate the origin of RH421 fluorescence changes without the complication of Na^+ or K^+ binding reactions.

The significance of the findings presented here goes beyond elucidating the mechanism of a non-physiological membrane probe. If the response mechanism of the dye can be discovered, then this automatically provides information on the "signal" that the protein is sending out. Thus, the investigation allows mechanistic detail regarding the function and regulation of the Na^+,K^+-ATPase to be gained. To be precise, we will show evidence that the response of RH421 is due to an interaction of the protein's lysine-rich cytoplasmic N-terminus with the neighbouring lipid membrane. This represents an important new aspect of the Na^+,K^+-ATPase mechanism which has up to now been largely overlooked, in part because the N-terminus has not been resolved in any of the published crystal structures of the protein.

2. Materials and methods

2.1 Enzyme and reagents

Na^+,K^+-ATPase–containing open membrane fragments from shark rectal glands were purified essentially as described by Skou and Esmann [40]. Na^+,K^+-ATPase-containing open membrane fragments from pig kidney were purified as described by Klodos et al. [41]. Na^+,K^+-ATPase–containing open membrane fragments from the supraorbital salt gland of juvenile ducks were purified as described by Pratap et al. [42]. The specific ATPase activity of the shark preparation at 37 ºC and pH 7.4 was measured according to Ottolenghi [43] to be 1746 μmol ATP hydrolysed h^{-1} (mg of protein)$^{-1}$ at saturating substrate concentrations. The activity of the pig preparation, measured by the same method, was 1086 μmol ATP hydrolysed h^{-1} (mg of protein)$^{-1}$. Typical activities of the duck preparation, measured by a fluorescence-coupled enzyme assay [44, 45], are >3300 μmol ATP hydrolysed h^{-1} (mg of protein)$^{-1}$. The protein concentration of the shark preparation was 4.46 mg mL^{-1} according to the Peterson modification [46] of the Lowry method [47] using bovine serum albumin as a standard. The protein concentration of the pig preparation was determined by the same procedure to be 6.17 mg mL^{-1}. The protein concentration of the duck preparation was determined by a modified Lowry method [47], as described previously [42], to be 5.2 mg mL^{-1}.

N-(4-Sulfobutyl)-4-(4-(*p*-(dipentylamino)phenyl)butadienyl)-pyridinium salt (RH421) was obtained from Molecular Probes (Eugene, OR) and used without further purification. RH421 was added to Na^+,K^+-ATPase-containing membrane fragments or to lipid vesicles from an ethanolic stock solution. The dye spontaneously partitions into membranes.

For measurements of the reaction of inorganic phosphate, P_i, with the Na^+,K^+-ATPase, tris(hydroxymethyl)amino)methane (Tris) was added to a 100 mM stock solution of orthophosphoric acid to reach a pH of 7.4. Dilutions of a range of P_i concentrations were then

prepared in a Tris buffer (30 mM Tris, 10 mM $MgCl_2$, 1 mM EDTA). The pH of the buffer was adjusted to 7.4 with HCl.

The origins of the reagents used were: Tris (minimum 99.9%, Sigma, Deisenhofen, Germany), NaCl (suprapure, Merck, Kilsyth, Australia), $MgCl_2 \cdot 6H_2O$ (analytical grade, Merck, Darmstadt, Germany), EDTA (99%, Sigma), ATP magnesium salt$\cdot 5.5H_2O$ (~97%, Sigma), orthophosphoric acid (85%, suprapure, Merck), poly-L-lysine hydrochloride (MW 15,000 – 30,000 g mol^{-1}, Sigma), ethanol (analytical grade, Merck), and HCl (0.1 N Titrisol solution, Merck).

Dimyristoylphosphatidylcholine (DMPC) was obtained from Avanti Polar Lipids (Alabaster, AL). Unilamellar vesicles were prepared by the ethanol injection method described in detail elsewhere [48, 49].

2.2 Fluorescence spectrophotometer measurements

Fluorescence measurements were carried out with either an F-4500 fluorescence spectrophotometer (Hitachi, Tokyo, Japan) or RF-5301 PC spectrofluorophotometer (Shimadzu, Kyoto, Japan) using quartz cuvettes. The temperature was maintained at 24 ºC via a circulating water bath. λ_{ex} was 577 nm (bandwidth 20 nm) with an OG530 filter (Schott) in the excitation path. λ_{em} was 670 nm (bandwidth 10 nm) with an RG645 filter (Schott) in front of the photomultiplier. The response time of the instrument was set to either 0.5 or 0.01 seconds.

The relative fluorescence change, $\Delta F/F_0$, of membrane-bound RH421 associated with interaction of P_i with the Na^+,K^+-ATPase was determined by measuring the change in fluorescence, ΔF, of a suspension of open Na^+,K^+-ATPase-containing membrane fragments (24 μg/ml) noncovalently labelled with RH421 (270 nM) following P_i addition and then dividing ΔF by the fluorescence prior to P_i addition, F_0. Measurements were performed in a

solution containing 30 mM Tris, 10 mM $MgCl_2$, and 1 mM EDTA. The pH was adjusted to 7.4 with HCl.

Under these solution conditions, the presence of Mg^{2+}, a co-factor for phosphorylation, allows the Na^+,K^+-ATPase to undergo phosphorylation. The absence of both Na^+ and K^+, inhibits dephosphorylation [50] and hence in the solutions described above the enzyme accumulates in a phosphorylated state.

2.3 UV-visible absorbance spectrophotometer measurements

UV-visible absorbance measurements were carried out with a UV-2450 UV-visible spectrophotometer (Shimadzu, Kyoto, Japan) using quartz semi-micro cuvettes. The temperature was maintained at 24 ºC via a circulating water bath. To eliminate scattering contributions to the measured absorbance spectra of membrane-bound RH421, Na^+,K^+-ATPase-containing membrane fragments and poly-L-lysine were added to the reference cuvette as well as to the sample cuvette. The bandwidth used was 5 nm.

2.4 Stopped-flow spectrofluorimetry

Stopped-flow experiments were carried out using either an SF-61 or SF-61SX2/s stopped-flow spectrofluorimeter from TgK Scientific (Bradford on Avon, UK) as described previously [51]. To improve the signal/noise ratio, the electrical time constant of the instrument was set to a value of 0.01 s, still a factor of over 100 faster than the fastest fluorescent transients observed here, and typically 6-9 experimental traces were averaged before the k_{obs} values were evaluated. To avoid interference from photochemical reactions [51, 52] of the dye, neutral density filters, either NG10% (Schott, Mainz) for measurements on shark enzyme or NG10% plus NG50% for pig enzyme, were placed in the excitation light

beam. This reduced the k_{obs} of the dye's photochemical reaction to a value of 0.03-0.04 s^{-1}, a factor of at least 10 slower than the observed Na^+,K^+-ATPase-related fluorescence transients.

The kinetics of Na^+,K^+-ATPase conformational changes were investigated at 24 ºC in the stopped-flow apparatus by mixing Na^+,K^+-ATPase (labelled with RH421) with an equal volume of a phosphate solution. Both solutions were prepared in the same solution containing 30 mM Tris, 10 mM $MgCl_2$, and 1 mM EDTA. No change in Mg^{2+} concentration occurred on mixing. The protein and dye concentrations after mixing were the same as in the fluorescence spectrophotometer measurements.

2.5 Kinetic data fitting

The reaction of P_i with the Na^+,K^+-ATPase can be considered to involve three steps:

$$E1 \underset{k_{-1}}{\overset{k_1}{\rightleftharpoons}} E2$$

$$E2 + P_i \overset{K_2}{\rightleftharpoons} E2 \cdot P$$

$$E2 \cdot P \overset{K_3}{\rightleftharpoons} E2P$$

The first step is the conformational change between E1 and E2 (with forward and backward rate constants k_1 and k_{-1}, respectively), the second step represents the second order binding reaction of P_i to the E2 conformation, producing E2·P, (with an equilibrium constant K_2) and the third step is the actual phosphorylation in which the phosphate is covalently linked to the protein, producing E2P (with an equilibrium constant K_3). If one assumes that the conformational change is the slowest of the three steps and that the second two are in equilibrium on the timescale of the conformational change, one can derive an equation relating k_{obs} to the P_i concentrations, the rate constants for the conformational change and the equilibrium constants for the other two reactions.

The relaxation of the E1/E2 equilibrium into a new equilibrium position following the addition of P_i can be described by the following differential rate equation:

$$-\frac{d\Delta E1}{dt} = k_1 \Delta E1 - k_{-1} \Delta E2 \qquad (1)$$

where ΔE1 and ΔE2 are the deviations of the concentrations of E1 and E2 from their final equilibrium positions. Based on the assumption that there are no other enzyme species present apart from those shown in the above reaction, the concentration deviations are all linked by:

$$\Delta E1 + \Delta E2 + \Delta E2 \cdot P + \Delta E2P = 0 \qquad (2)$$

Because the second two steps in the reaction scheme are considered to be in equilibrium on the timescale of the conformational change, one can express both ΔE2·P and ΔE2P in terms of ΔE2 based on the law of mass action as follows:

$$\Delta E2 \cdot P = K_2 [P_i] \Delta E2 \qquad (3)$$

$$\Delta E2P = K_2 K_3 [P_i] \Delta E2 \qquad (4)$$

Substituting these two expressions into Eq. 2 for ΔE2·P and ΔE2P and rearranging yields:

$$\Delta E2 = -\frac{\Delta E1}{1 + K_2 [P_i](1 + K_3)} \qquad (5)$$

Finally, substituting ΔE2 from Eq. 5 into the differential rate equation, Eq. 1, it can be shown that the observed rate constant, k_{obs}, for the relaxation of the conformational equilibrium is given by:

$$k_{obs} = k_1 + \frac{k_{-1}}{1 + K_2 [P_i](1 + K_3)} \qquad (6)$$

Because $[P_i]$ is in the denominator of the second term on the right hand side of this equation, it predicts a decrease in the value of k_{obs} as $[P_i]$ increases, as has been experimentally observed, from a value of $k_1 + k_{-1}$ at infinite dilution of P_i to a value of k_1 at an infinite

concentration of P_i. Eq. 6 is in the same form as an equation previously derived by Cornelius et al. [39] to describe the kinetics of back-door phosphorylation of the Na^+,K^+-ATPase, although the method of derivation is different.

Nonlinear least-squares fitting of Eq. 6 to the P_i concentration dependence of the k_{obs} values determined by stopped-flow was performed using Origin 6.0 (Microcal Software, Northampton, MA).

2.6 Quantum-mechanical calculations

All *ab initio* calculations have been performed with the Gaussian 09 code [53], using default procedures except for those noted below. First, the ground-state geometry of RH421 was optimized using the M06-2X exchange-correlation DFT functional [54] combined with the 6-311G(d,p) atomic basis set. These calculations were performed with tighten SCF convergence threshold (10^{-10} au), force optimization threshold (10^{-5} au on RMS forces) and an improved DFT integration grid, the so-called *ultrafine* (99,590) grid. Second, the vibrational spectrum was determined at the same level of theory. This allowed us to ascertain that the optimised structure is a true minimum of the potential energy surface (absence of imaginary frequency). Third, the vertical transition energies to the lowest singlet excited-state have been determined with TD-DFT using the same M06-2X functional but a larger atomic basis set, namely 6-311+G(2d,p). In all steps, the surrounding effects were described using the SMD continuum model [55] and choosing water as solvent. The linear-response regime in its *non-equilibrium* limit was applied for the TD-DFT part of the calculation. The choice of water is based on experimental results showing that the λ_{max} of RH421 in water and when membrane-bound are quite similar, i.e. within 5 nm of each other [56]. To quantify the impact of a positive charge on RH421, we have determined the optical spectra using a Na^+ ion placed at various locations in the vicinity of the dye.

2.7 Molecular dynamics simulations

To examine the state-dependent influence of the Na^+,K^+-ATPase on lipid bilayer thickness, we have carried out molecular dynamics (MD) simulations. Available structures for the pig Na^+,K^+-ATPase in E1 and E2 states (PDB codes 3WGU [57] and 3B8E [58], respectively) were embedded in bilayers of 1,2-dioleoyl-*sn*-glycero-3-phosphocholine (DOPC) lipids (447 and 550 lipids respectively) immersed in 150 mM NaCl solution using explicit TIP3P water molecules, with the E1 system containing 295,312 atoms and E2 containing 299,532 atoms. Systems were built with CHARMM-GUI [59], and then equilibrated using NAMD 2.9 [60] with the CHARMM36 force field [61, 62]. Temperature was maintained at 303.15 K using a Langevin thermostat and pressure maintained at 1 atm using the Nose-Hoover Langevin piston method [63] with hexagonal periodic boundaries. All bonds to hydrogen atoms were maintained using the SHAKE algorithm [64]. Electrostatic interactions were computed using Particle Mesh Ewald [65] with grid spacing of 1 Å. Non-bonded pair lists were recorded to 16 Å with real space cutoff 12 Å using energy switching from 10 Å. Each system has been run for 100 ns, with the last 50 ns used for analysis.

Lipid bilayer thickness has been analysed based on the difference in the positions of carbonyl C atoms within each leaflet, representing the membrane hydrophobic core thickness [66]. Each protein was oriented with trans-membrane domain at the origin and directed such that the *xy* projection of the vector connecting the centre of mass (COM) of residues 90 to 110 (within αM1) and 123 to 137 (within αM2) and the COM of residues 845 to 868 (within αM7) and residues 910 to 928 (within αM8) coincides with the y axis. For 2-D maps of carbonyl C to C membrane deflection, thickness was computed on a 5 × 5Å *xy* grid, offset by removing the average far from the protein ($50 \leq r < 100$ Å) to reveal the lipid bilayer deflection due to the protein. For 1-D axially symmetrised plots of carbonyl deflection, the

difference in average positions of carbonyl C atoms was computed within concentric shells (between radius $r - 1$ and $r + 1$Å). All error bars are standard error of means obtained from three independent blocks of trajectories.

3. Results

3.1 Effect of P_i on the fluorescence of RH421-labelled Na^+,K^+-ATPase-containing membrane fragments

Addition of 6 mM P_i to a suspension of Na^+,K^+-ATPase-containing membrane fragments from shark rectal gland noncovalently labelled with RH421 causes an increase in fluorescence of approximately 80% (see Fig. 1). The magnitude of the fluorescence change was found to follow a hyperbolic dependence on the P_i concentration used. 6 mM P_i corresponds to a saturating concentration. In contrast to previously published data using rabbit kidney Na^+,K^+-ATPase [38], there was no initial rapid jump in fluorescence. The fluorescence change is monophasic, in agreement with other results obtained using shark rectal gland enzyme [39], with a time constant of approximately 3.4 seconds (corresponding to an observed rate constant of 0.29 s^{-1}).

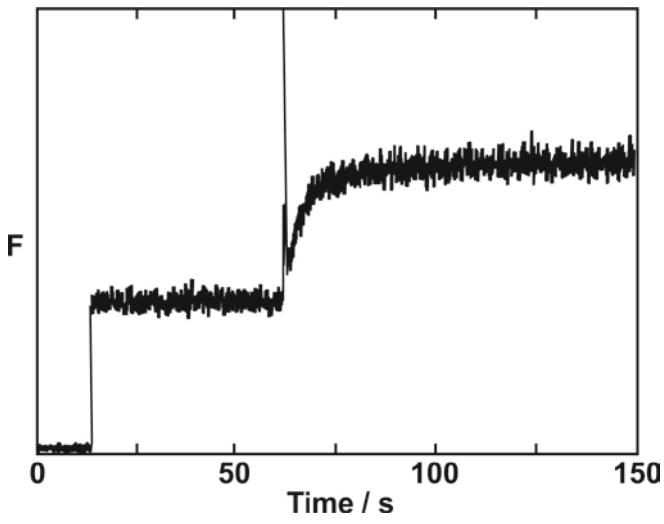

Figure 1: RH421 fluorescence change accompanying the addition of 6 mM of tris phosphate to shark rectal gland Na^+,K^+-ATPase. The Na^+,K^+-ATPase and RH421 concentrations were 24 μg/ml and 270 nM, respectively. The measurements were performed in a buffer containing 30 mM Tris, 10 mM $MgCl_2$, and 1 mM EDTA, pH 7.4, 24ºC. The fluorescence increase at approximately 15 seconds is due to the addition of RH421 to the Na^+,K^+-ATPase-containing membrane fragments and the incorporation of the dye into the membrane. The fluorescence increase due to phosphorylation of the protein can be seen after 65 seconds, when P_i was added. The fluorescence intensity is in arbitrary units.

To test whether the difference between the kinetic time course observed using shark enzyme and that obtained with rabbit kidney enzyme [38] may be due to the enzyme source, we also carried out the same experiment with enzyme derived from mammalian kidney, in this case pig kidney Na^+,K^+-ATPase. Although the change in fluorescence was much smaller than with the shark enzyme (only 10-15%), the change was again monophasic (see Fig. 2). Again no evidence for an initial rapid jump in fluorescence could be observed. The amino acid sequences of the catalytic α-subunits of the rabbit and pig kidney Na^+,K^+-ATPases show 97% identity and 99% homology. Therefore, it seems very unlikely that the different behavior observed in studies with rabbit kidney enzyme [38] is due to differences in protein structure. A possibility is that it is related to the method of P_i addition. In the studies using rabbit kidney enzyme, P_i was added by releasing it photochemically from a caged complex using a UV laser flash rather than simply adding P_i to the cuvette. A potential problem of the photochemical method is that it introduces photochemical degradation products into the reaction mixture apart from phosphate itself.

If $MgCl_2$ is removed from the buffer, it was found that the fluorescence change on addition of P_i is completely abolished. This is consistent with Mg^{2+} acting as a necessary cofactor for protein phosphorylation, as it also does for phosphorylation by ATP.

In order to quantify the observed rate constants and their dependence on the P_i concentration more precisely, the reaction was further investigated using the stopped-flow fluorimeter.

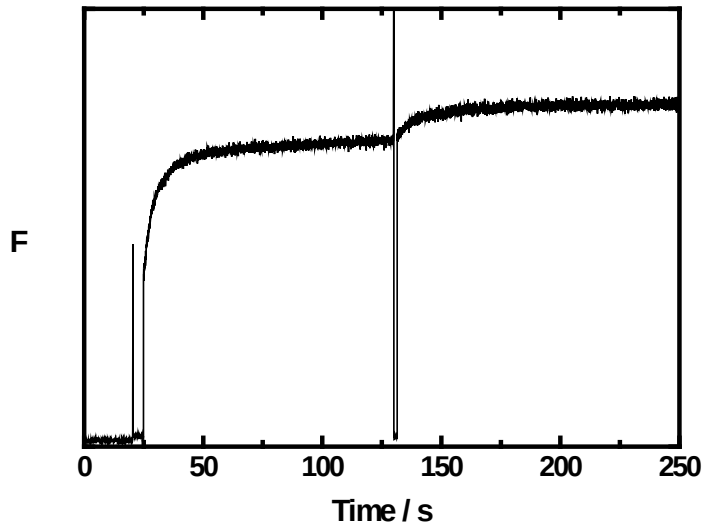

Figure 2: RH421 fluorescence change accompanying the addition of 6 mM of tris phosphate to pig kidney Na^+,K^+-ATPase. The Na^+,K^+-ATPase and RH421 concentrations were 25 μg/ml and 250 nM, respectively. The measurements were performed in a buffer containing 30 mM Tris, 10 mM $MgCl_2$, and 1 mM EDTA, pH 7.4, 24ºC. The fluorescence increase at approximately 25 seconds is due to the addition of RH421 to the Na^+,K^+-ATPase-containing membrane fragments and the incorporation of the dye into the membrane. The fluorescence increase due to phosphorylation of the protein can be seen after 130 seconds, when P_i was added. The fluorescence intensity is in arbitrary units.

3.2 Rates of P_i-induced stopped-flow fluorescence traces

An example of a fluorescence trace induced by mixing with P_i in the presence of Mg^{2+} ions in a stopped-flow fluorimeter is shown in Fig. 3. In contrast to the measurements in the steady-state fluorimeter, the kinetic traces measured via stopped-flow are biphasic, but only because of a very slow photochemical reaction of RH421 which causes an increase in fluorescence [51, 52]. Thus, there is still only a single phase due to the Na^+,K^+-ATPase. The reason the photochemical reaction isn't observed in the steady-state fluorimeter is because of the lower light intensity used there and because, in contrast to the stopped-flow, only a relatively small volume of the entire cuvette is irradiated. Thus, in the steady-state fluorimeter the dye is constantly diffusing in and out of the light beam, which reduces the likelihood of photochemical reactions. The observed rate constant, k_{obs}, for the Na^+,K^+-ATPase-related phase of the fluorescence transient was determined by fitting a double-exponential time function to the experimental stopped-flow data.

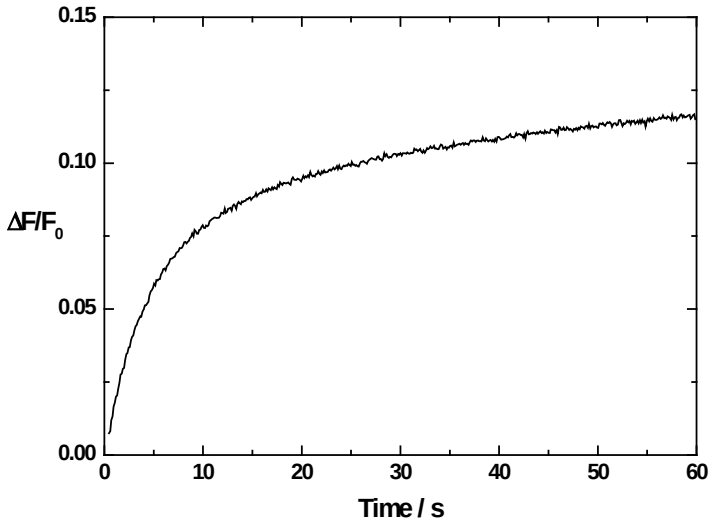

Figure 3: Stopped-flow fluorescence transient of pig kidney Na^+,K^+-ATPase non-covalently labeled with RH421 (125 nM after mixing). Na^+,K^+-ATPase (25 µg/ml after mixing) was rapidly mixed with an equal volume of tris phosphate (6 mM after mixing). The measurements were performed in a buffer containing 30 mM Tris, 10 mM $MgCl_2$, and 1 mM

EDTA, pH 7.4, 24ºC. The excitation and emission wavelengths were 577 nm and ≥665 nm (RG665 cutoff filter), respectively.

As the P_i concentration is increased, the kinetics of the RH421 fluorescence rise due to the activity of the Na^+,K^+-ATPase becomes slower. The value of k_{obs} decreases hyperbolically from an initial value of approximately 0.7 s^{-1} to a final value at high P_i concentrations of approximately 0.3 s^{-1} (see Fig. 4). Fitting of Eq. 6 to the experimental data yields the following values for the rate and equilibrium constants of the reaction scheme given under Materials and Methods: k_1 = 0.29 (± 0.02) s^{-1}, k_{-1} = 0.40 (± 0.02) s^{-1}, $K_2(1+K_3)$ = 0.99 (± 0.24) mM^{-1}.

From the kinetic data it is not possible to determine independent values of K_2 and K_3. However, the reciprocal of $K_2(1+K_3)$, which has the value 1.01 (± 0.25) mM, is equivalent to the half-saturating concentration of P_i necessary to produce a drop in k_{obs} to a value halfway between the limiting values of ($k_1 + k_{-1}$) and k_1. It is not simply the dissociation constant for P_i because it incorporates the thermodynamics of phosphorylation of the protein as well as phosphate binding.

From the ratio of the values of k_1 and k_{-1}, one can also calculate a value for the equilibrium constant, K_1 (= [E2]/[E1]), of 0.72 (± 0.07). Based on this value one can estimate that, prior to mixing with P_i, 58% of the enzyme should be in the E1 conformation and 42% in the E2 conformation.

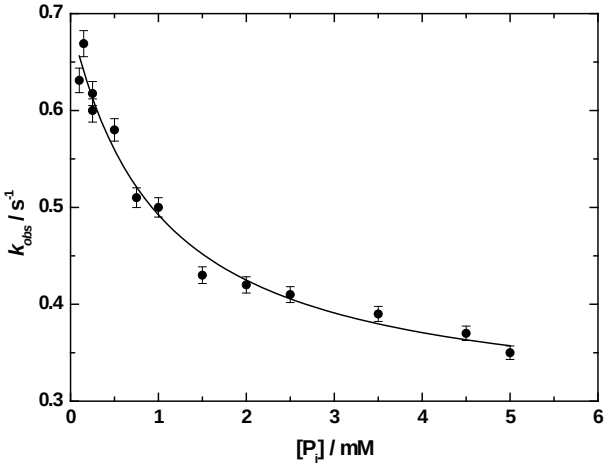

Figure 4: Dependence of the observed rate constant, k_{obs}, of the RH421 fluorescence change observed using shark rectal gland Na^+,K^+-ATPase on the concentration of P_i (after mixing). The solid line is a nonlinear least-squares fit of the data to Eq. 6. The fit parameters were : k_1 = 0.29 (± 0.02) s^{-1}, k_{-1} = 0.40 (± 0.02) s^{-1}, $K_2(1+K_3)$ = 0.99 (± 0.24) mM^{-1}. $K_2(1+K_3)$ corresponds to a $K_{0.5}$ of 1.01 (± 0.25) mM. The conformational equilibrium constant K_1 = [E2]/[E1] = k_1/k_{-1} = 0.72 (± 0.07). The Na^+,K^+-ATPase and RH421 concentrations after mixing were 24 μg/ml and 270 nM, respectively. The measurements were performed in a buffer containing 30 mM Tris, 10 mM $MgCl_2$, and 1 mM EDTA, pH 7.4, 24ºC.

3.3 Membrane hydrophobic thickness

In a previous publication [31] we suggested that the origin of RH421 fluorescence changes in Na^+,K^+-ATPase-containing membrane fragments might be protein-induced changes in the membrane hydrophobic thickness which could produce local changes in membrane dipole potential around the protein detectable by the probe. To test the feasibility of this hypothesis we have analyzed protein hydrophobic thicknesses in different protein conformations based on available X-ray crystal structures [57, 58] and MD simulations in lipid bilayers.

According to the Orientations of Proteins in Membranes (OPM) database (http://opm.phar.umich.edu/) [67], the hydrophobic thickness of pig Na^+,K^+-ATPase in the $E1P\cdot ADP\cdot 3Na^+$ state is 30.8 (± 1.1) Å based on the structure PDB:3WGU [57] and 31.0 (± 1.3) Å based on the structure PDB:4HQJ [68]. In the $E2\cdot P_i\cdot 2K^+$ state, according to the OPM database the available crystal structures indicate hydrophobic thicknesses of 31.9 (± 1.8) Å for shark Na^+,K^+-ATPase (PDB:2ZXE) [69] and 30.7 (± 0.9) Å for pig Na^+,K^+-ATPase (PDB:3B8E) [58]. Therefore, based on these crystal structures alone there doesn't appear to be a significant difference in hydrophobic thickness. However, the number of crystal structures available for the Na^+,K^+-ATPase is still very limited.

To obtain a more precise analysis of Na^+,K^+-ATPase hydrophobic thicknesses we have carried out MD simulations of both the $E1P\cdot ADP\cdot 3Na^+$ state and the $E2\cdot P_i\cdot 2K^+$ state of pig kidney enzyme based on the structures PDB:3WGU [57] and PDB:3B8E [58], respectively. Relaxation of the $E1P\cdot ADP\cdot 3Na^+$ and $E2\cdot P_i\cdot 2K^+$ states of the pig kidney Na^+,K^+-ATPase in lipid bilayers (see Fig. 5a) reveals statistically significant local perturbations of the membrane, with lipids displaced by the irregular protein surface. The time-averaged deflection of the bilayer is illustrated in Fig. 5b, demonstrating both thinning and thickening by several Å on different faces of the protein, with distinct distributions in the $E1P\cdot ADP\cdot 3Na^+$ (left; "E1") and $E2\cdot P_i\cdot 2K^+$ (right; "E2") states. Approximate locations of key trans-membrane helices in the figure suggest likely origins of the perturbations due to local mismatch. Key changes are associated with regions near helices αM2, αM9 and γM (left face of the figure), αM1 (top), αM10 (bottom), and βM (bottom right). While there is a generally similar pattern of lipid deflection in each state, we observe that lipids on the αM9-γM-αM10 face, particularly near αM10, are more positively displaced in the $E1P\cdot ADP\cdot 3Na^+$ state (i.e., causing a local increase in membrane hydrophobic thickness) and more negatively displaced in the $E2\cdot P_i\cdot 2K^+$ state, penetrating into the membrane surface (evident in Fig. 5a). This is

associated with a reduction in negatively displaced lipids around αM2-αM9, which appears to relate to tilting of the αM9 helix, as well as αM1 and αM2, but with a net overall negative deflection on the αM2-αM10 (left) face in going from the E1P·ADP·$3Na^+$ state to the E2·P_i·$2K^+$ state. On the opposite face of the protein, there is a reduction in positive deflection of lipids between αM1-βM, and shift in the positions of negatively deflected lipids near βM, which seem to relate to noticeable tilt in helix βM between the E1P·ADP·$3Na^+$ and E2·P_i·$2K^+$ states. The net effect of these lipid deflections due to protein conformational change is a negative deflection of lipids in the vicinity of the protein by 2–3 Å, as seen in the axially averaged plots of Fig. 5c. Thus, while the differences in apparent hydrophobic thicknesses of the trans-membrane regions in the crystal structures for E1P·ADP·$3Na^+$ and E2·P_i·$2K^+$ states are not substantial, relaxation of the lipid bilayer around each protein has uncovered local perturbations, approaching 10% of bilayer thickness on average.

Based on a recent theoretical treatment of the effects of membrane dipole potential, ψ_d, on ion pumps [35], a local increase in membrane thickness would be expected to perturb lipid packing, increasing lipid packing density and ψ_d. An increase in ψ_d is known to cause a blue shift in the RH421 fluorescence excitation spectrum [10], which would result in a drop in fluorescence intensity when the fluorescence is excited on the red edge of the excitation spectrum, as is normally done. Although the hydrophobic thickness changes appear to be in a direction consistent with the dye response, it seems unclear that a change in hydrophobic thickness of ≤ 10% could completely explain the dye response, where relative fluorescence intensity changes exceeding 100% have been observed when RH421 has been used as a probe for the Na^+,K^+-ATPase [31]. Nevertheless, the hydrophobic thickness changes are particularly interesting and could in part explain the sensitivity of Na^+,K^+-ATPase kinetics to the presence of cholesterol in the membrane, which is known to significantly increase ψ_d [35]. As described in detail elsewhere [35], through its effect on ψ_d, cholesterol would be expected

to preferentially stabilize ion pump states with a small hydrophobic thickness relative to those with a large hydrophobic thickness, thus leading to changes in the activation energies of individual partial reactions and hence a modulation of the overall enzymatic turnover.

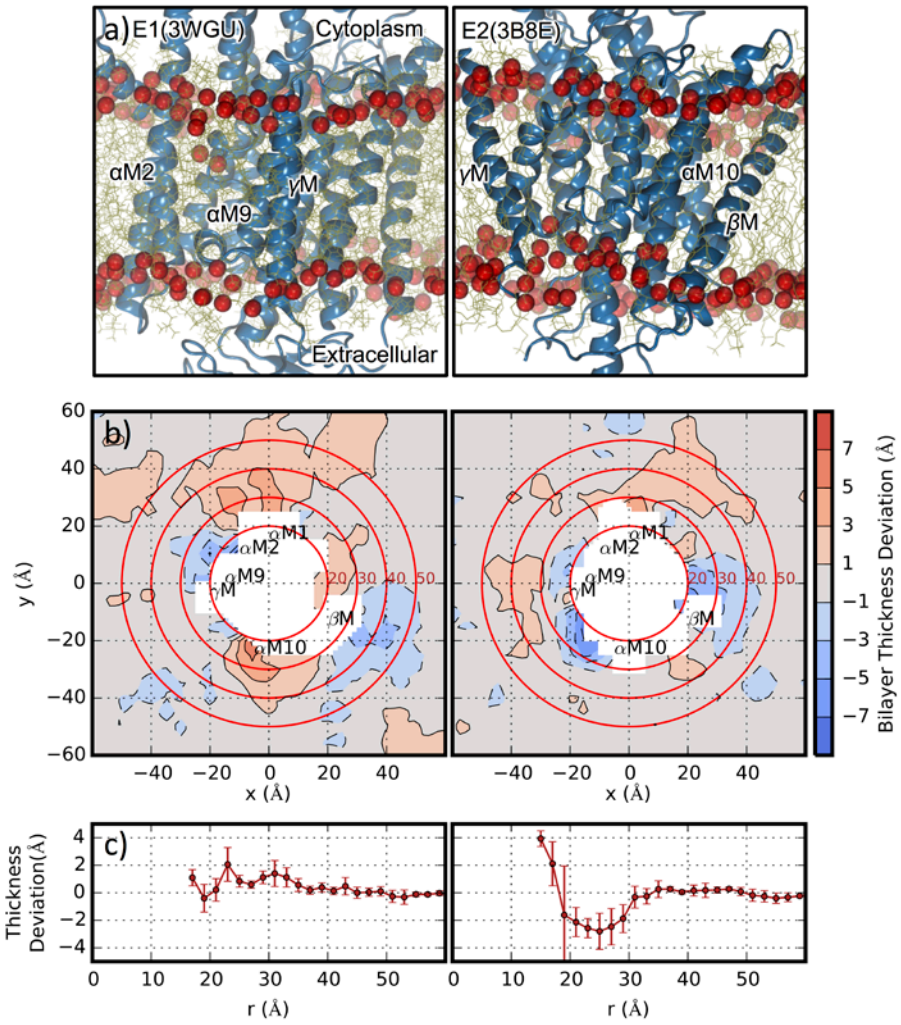

Figure 5: a) Na^+,K^+-ATPase in a DOPC lipid bilayer in E1P·ADP·$3Na^+$ (PDB:3WGU; left) and E2·P_i·$2K^+$ (PDB:3B8E, right) states, showing only the region near the trans-membrane domain to illustrate membrane deformation. Protein is shown as blue ribbons, lipid carbonyl carbon atoms as red spheres, lipid tails as yellow sticks, and electrolyte is not shown for clarity. b) Map of lipid carbonyl C to C thickness deviation (relative to distant membrane; 29.2 ± 0.2 Å in E1P·ADP·$3Na^+$ and 29.6 ± 0.3 Å in E2·P_i·$2K^+$ state) on a 5.0 Å grid, as

viewed from the cytoplasmic side. Approximate locations of some helices of interest are indicated (see text). c) Axially averaged bilayer thickness deviation as function of distance *r* from the protein COM.

Further evidence suggesting that membrane perturbation may not be a major factor in the RH421 response mechanism can be found in a comparison of the magnitudes of the dye's fluorescence response to different P-type ATPases. Whereas RH421 and other dyes of the RH class produce relatively large responses to partial reactions of the Na^+,K^+-ATPase and the H^+,K^+-ATPase [15, 17-24, 70], only tiny responses have been observed with the sarcoplasmic reticulum (SR) Ca^{2+}-ATPase [71]. In order to obtain fluorescence changes sufficiently large to analyse, Butscher et al. [71] had to change to a different class of dye, lacking a negatively charged sulfonate group and incorporating a neutral isothiocyanate group instead. The same class of dyes has subsequently been used in further studies on the SR Ca^{2+}-ATPase [19, 72, 73]. Considering the similarities in mechanisms and transmembrane domain structures of these three P-type ATPases, it seems unlikely that the large responses seen from the RH dyes when they are used in studies on the Na^+,K^+-ATPase or H^+,K^+-ATPase are due to changes in membrane structure arising from transmembrane domain conformational changes, because otherwise one might expect a similar response with the SR Ca^{2+}-ATPase. Based on the differences in response of RH421 to the different ATPases, a more likely origin of the response may perhaps be found from amino acid sequence comparisons of the Na^+,K^+-ATPase and the H^+,K^+-ATPase with the SR Ca^{2+}-ATPase (see Section 3.5).

3.4 Interaction of poly-L-lysine with membrane-bound RH421

While changes in protein hydrophobic thickness may play some role in the RH421 response to Na^+,K^+-ATPase conformational changes, the possibility that the dye is directly

interacting with the protein needs to be considered. Earlier experiments have already shown that RH421 is able to interact directly with proteins, most likely via its negatively charged sulfonate group through an interaction with positively charged lysine or arginine amino acid residues [36, 37]. From trypsin digest experiments it is known that significant movements of the N-terminal sequence of the α-subunit of the Na^+,K^+-ATPase accompany the E2-E1 conformational transition [74-76]. The N-terminus is particularly lysine-rich and has been proposed to act as a movable ion-selective gate during cation binding and occlusion [77]. Recent studies on the effect of ionic strength on the E2-E1 conformational transition of the Na^+,K^+-ATPase have also been explained in terms of the screening of an electrostatic interaction of the N-terminus with the cytoplasmic surface of the surrounding membrane [78].

Therefore, to investigate whether RH421 could be interacting with lysine residues of the N-terminus we measured the effect of adding poly-L-lysine to RH421 bound to Na^+,K^+-ATPase-containing membrane fragments on the dye's visible absorbance spectrum (see Fig. 6A). Poly-L-lysine was found to cause a significant red shift in the dye's spectrum and a decrease in absorbance. At a poly-L-lysine concentration of 3.8 μg/ml (see Fig. 6A), the red shift amounts to only just over 1 nm. However, as the poly-L-lysine concentration is increased, the RH421 absorbance spectrum shifts further to the red. At a poly-L-lysine concentration of 7.6 μg/ml, λ_{max} occurs at 500 nm, a red shift of approximately 13 nm relative to zero poly-L-lysine. The spectral changes observed at approximately 3.8 μg/ml poly-L-lysine parallel those which occur when the Na^+,K^+-ATPase is phosphorylated by ATP in the presence of Na^+ and Mg^{2+} ions (see Fig. 6B). Experiments in which poly-L-lysine were added to RH421 bound to DMPC vesicles also showed a red shift in the dye's spectrum, but the effect was much smaller than that observed with Na^+,K^+-ATPase-containing membrane fragments, i.e. maximal 1 nm. The difference in the magnitude of the effect is most likely due

to different lipid compositions. The activity of the Na^+,K^+-ATPase has long been known to be dependent on the presence of anionic lipids [79, 80], in particular phosphatidylserine, which are known to enhance the interaction of membranes with poly-L-lysine and lysine-containing oligopeptides [81, 82].

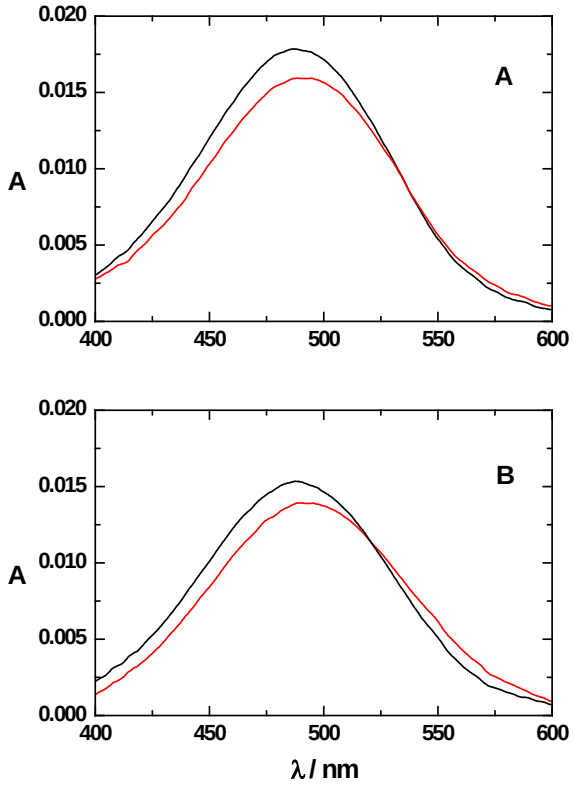

Figure 6: Visible absorbance spectra of RH421 (250 nM) bound to duck Na^+,K^+-ATPase-containing membrane fragments before (black curve) and after (red curve) adding either 3.8 mg/ml poly-L-lysine (panel A) or 0.5 mM ATP (panel B) to the suspension. The measurements were performed in a solution containing 30 mM Tris, 150 mM NaCl, 1 mM EDTA, and 5 mM $MgCl_2$, pH 7.2, 24°C.

3.5 Amino acid sequence analysis

Because of the evidence described in the previous section indicating that the N-terminus of the Na^+,K^+-ATPase is likely to be involved in the RH421 response, we decided to carry out a comparison on the amino acid sequences of the N-termini of the Na^+,K^+-ATPase, the gastric H^+,K^+-ATPase and the SR Ca^{2+}-ATPase. As described in Section 3.5, it is known that RH421 responds with significant fluorescence changes to partial reactions of the Na^+,K^+-ATPase and the H^+,K^+-ATPase, but only with minimal changes to partial reactions of the Ca^{2+}-ATPase.

The entire sequences of the SR Ca^{2+}-ATPase and the catalytic α-subunits of the Na^+,K^+- and H^+,K^+-ATPases were first aligned within the MEGA7 suite of evolutionary genetics programs [83]. For the analysis the sequences from rabbit (*Oryctolagus cuniculus*) were chosen, because this species has been used for all of the X-ray crystal structure determinations of the SR Ca^{2+}-ATPase. The alignment of the N-terminal segments (i.e., up to the start of the first transmembrane helix) of the three proteins is shown in Fig. 7. One obvious difference is that the N-terminus of the SR Ca^{2+}-ATPase is much shorter than that of both the Na^+,K^+-ATPase and the H^+,K^+-ATPase. Its length is reduced by 50% compared to the H^+,K^+-ATPase and by 45% compared to the Na^+,K^+-ATPase. Another significant difference is in the lysine content. The N-terminus of the SR Ca^{2+}-ATPase contains only 4 lysine (K) residues, whereas the Na^+,K^+-ATPase has 11 and the H^+,K^+-ATPase 12 (lysine residues in the propeptide sequence of the first five amino acids which is deleted prior to membrane insertion in the Na^+,K^+- and H^+,K^+-ATPase have been ignored). Furthermore, many of the lysines of the Na^+,K^+-ATPase and the H^+,K^+-ATPase occur as consecutive blocks.

Although not conclusive proof, the significant differences in the N-terminus between the Na^+,K^+- and H^+,K^+-ATPases and the SR Ca^{2+}-ATPase is consistent with the idea that the N-terminus could be responsible for the minimal response of RH421 to the activity of the SR

Ca^{2+}-ATPase. Another possible contributing factor, however, could be different membrane compositions of the enzymes, since the SR Ca^{2+}-ATPase is located in a cell organelle, whereas the Na^+,K^+- and H^+,K^+-ATPases are both situated in the plasma membrane.

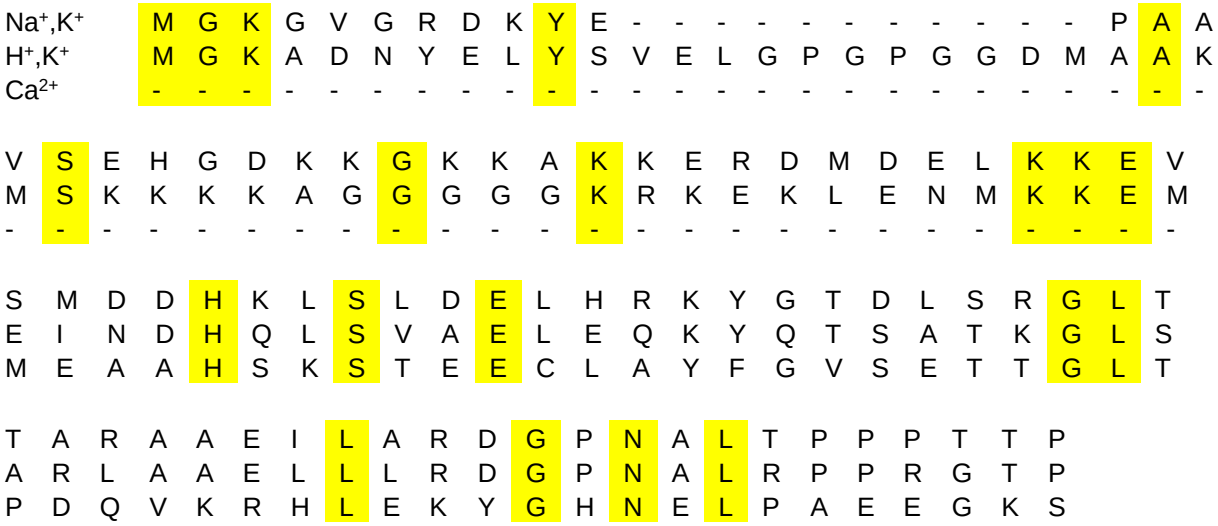

Figure 7: Amino acid sequence alignment of the N-termini of the α-subunit of the Na^+,K^+-ATPase, the α-subunit of the gastric H^+,K^+-ATPase and the SR Ca^{2+}-ATPase. All sequences were from rabbit (*Oryctolagus cuniculus*). Conserved residues are highlighted in yellow.

3.6 Quantum-mechanical calculations

To test the feasibility of neutralisation of the dye's negatively charged sulfonate group by binding of positively-charged lysine residues of the protein's N-terminus to the membrane surface, we first determined the transition energies for RH421 before and after protonation of its sulfonate group. Experimentally this cannot be done, because titration of the dye leads to protonation at one of its nitrogen atoms before protonation of the sulfonate. This theoretical calculation allows the effect of removal of the sulfonate negative charge on the UV/visible

absorbance of RH421 to be predicted. Association of a positive charge from a lysine residue of the N-terminus would be expected to have a similar effect.

In the vertical approximation, calculations yield λ_{max} values of 453 and 456 nm before and after sulfonate neutralisation, respectively. If the sulfonate is made to interact with a Na^+ cation whose position is optimised, a λ_{max} of 455 nm is obtained, i.e., very similar to the value obtained on protonation of the sulfonate group. As expected, the value of 453 nm does not perfectly fit with the experimental λ_{max} of RH421 in water, which is at 485 nm [56]. The main reasons for this difference are most likely to be, on the one hand, the neglect of vibronic effects in the calculation, and, on the other hand, the cyanine-nature of the excited-state of RH421 [84]. Nevertheless, the difference in the calculated transitions energies for the protonated and unprotonated forms of the dye, 145 cm^{-1}, can be used to predict the shift in λ_{max} that one would expect due to sulfonate neutralisation. Experimentally, when RH421 is bound to Na^+,K^+-ATPase-containing membrane fragments with the protein in the E1 conformation the λ_{max} of the dye occurs at 487 nm (see Fig. 6). Based on the theoretical calculations, if the response of the dye to conversion of the enzyme into the E2P conformation were due to neutralisation of the dye's sulfonate group by positive charges on the protein's N-terminus, one could expect a decrease in energy of the dye's electronic transition of 145 cm^{-1}, which would correspond to a final λ_{max} of ca. 490 nm. To within an accuracy of half a nanometre, this is in complete agreement with the experimentally observed value (see Fig. 6B).

To further investigate the effect of positive charge on the UV/visible absorbance spectrum of RH421 we also carried out calculations of the effect of a Na^+ ion at different distances from the molecule and different positions along its long axis. Here we would like to stress that, when bound to Na^+,K^+-ATPase-containing membrane, we do not think that RH421 is detecting an electric field from bound Na^+ ions, because this would contradict the

calculations published by Mares et al. [31]. In the calculations shown here we are simply using the Na^+ ion as a source of positive charge to investigate the magnitude and direction of the shift in the dye's absorbance spectrum when positive charge is located at different positions close to the dye. Bearing in mind that in the unperturbed state (i.e., no positive charge anywhere near the dye) the calculated λ_{max} was 453 nm, the results of the calculations shown in Fig. 8 indicate that the movement of a positive charge towards the dye perpendicular to its long axis causes a red shift of its absorbance spectrum and a slight decrease in its absorbance intensity (reflected in the oscillator strength values, *f*) as long as the positive charge is located at a depth no deeper than the second carbon atom below the dye's pyridinium ring. If the positive charge is moved to a position in line with the first carbon of the aniline ring or, even further down, to the amino nitrogen, the calculations show (see Fig. 8) that one would expect a reversal of the trend, i.e., a blue shift and a slight increase in absorbance intensity due to interaction with positive charge. Experimental results indicate that in fact a red shift and a decrease in absorbance of RH421 bound to Na^+,K^+-ATPase-containing membrane fragments is caused by the addition of positively-charged poly-L-lysine (see Fig. 6A) or ATP (see Fig. 6B). The theoretical calculations, therefore, suggest that poly-L-lysine and the lysine-rich N-terminus are not penetrating very deeply into the membrane, but rather interacting with the membrane surface, probably at the level of the lipid headgroups.

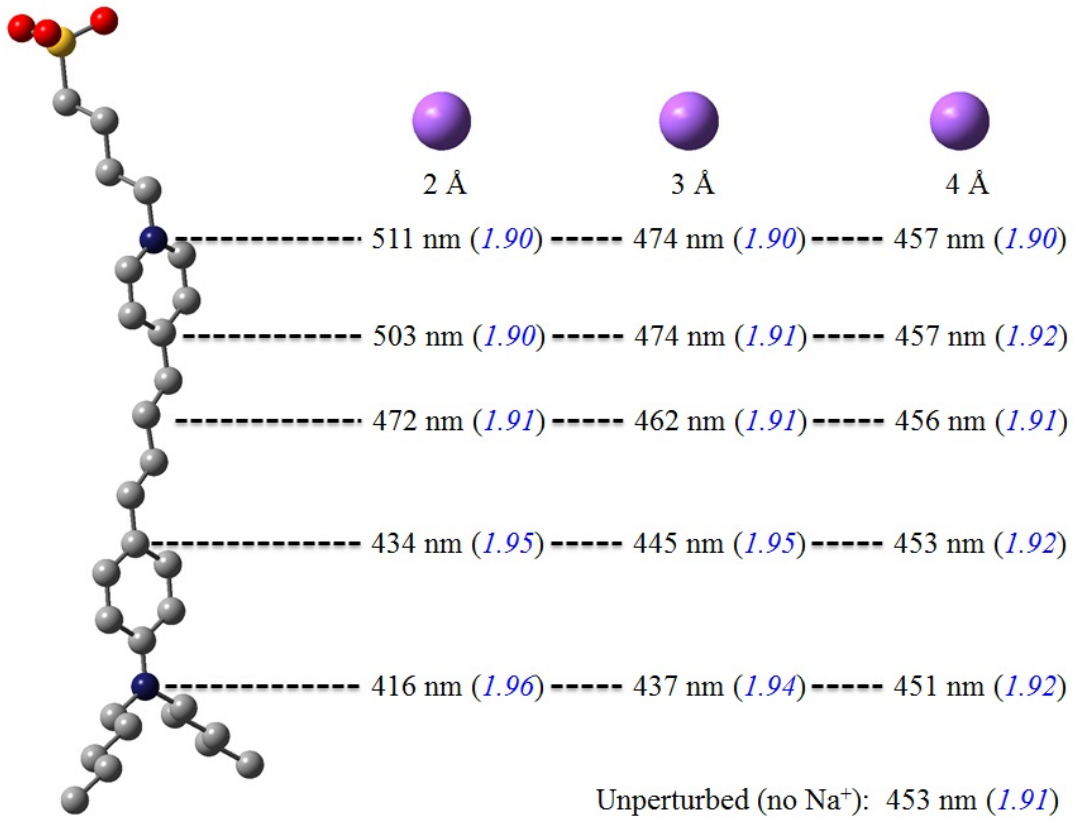

Figure 8: Effect of positive charge (introduced via a Na^+ ion) on the λ_{max} and the oscillator strength, *f*, of RH421 (H atoms omitted for clarity). Calculations were done by moving the Na^+ ion along axes perpendicular to the long axis of the RH421 molecule at the level of the atoms highlighted in red. Three different distances from these atoms were used: 2, 3 and 4 Å. The calculated λ_{max} values are given (in nm) in black. The corresponding *f* values are given in blue in italics.

4. Discussion

The primary goal of this paper is to determine the origin of the fluorescence response of the probe RH421 to reactions of the Na^+,K^+-ATPase. The rationale behind this is that, if we understand the response of the dye, then we will also understand the signal that the protein is sending out and thus gain valuable information regarding the interaction of the Na^+,K^+-ATPase with its surrounding membrane. This expectation indeed was verified by the

results obtained. Potentially the information gained could be of relevance also to other ion pumps and membrane proteins in general.

In a recent publication [31] we provided both experimental and theoretical data showing that RH421 is unlikely to be directly detecting electric field strength changes in the membrane originating from the transported Na^+ and K^+ ions, and we suggested that the protein conformational changes associated with ion occlusion within the protein could instead be responsible. To further investigate this hypothesis, here we first studied phosphorylation of the Na^+,K^+-ATPase by inorganic phosphate, a reaction which occurs in the complete absence of Na^+ and K^+ ions.

Phosphorylation of the Na^+,K^+-ATPase by inorganic phosphate, P_i, causes a significant increase in RH421 fluorescence (see Figs. 1-3). However, a series of coupled reactions are occurring, i.e., noncovalent phosphate binding to a binding site within the protein, the actual phosphorylation where phosphate is covalently linked to the protein, and a relaxation of the enzyme's E1/E2 conformational equilibrium (see the reaction scheme under Materials and Methods). Therefore, we must carefully consider which of these reactions could be responsible for the fluorescence change. To do this we must first establish the relative rates of the three reactions. Experimentally it has been found (see Fig. 4) that the k_{obs} of the RH421 fluorescence response decreases with increasing P_i concentration. This is consistent with the relaxation of the E1/E2 equilibrium being the slowest step in the sequence of reactions (see section 2.4 Kinetic data fitting under Materials and Methods). If the observed kinetics were due to second order P_i binding one would expect a linear increase in k_{obs} with increasing P_i concentration. If the observed kinetics were due to the phosphorylation reaction, then one should observe a hyperbolic increase in k_{obs} with increasing P_i concentration. A slow relaxation of a pre-existing E1/E2 equilibrium is the only reaction we can imagine which is consistent with the observed kinetics. This is so far in full agreement

with previous interpretations of the kinetics of P_i phosphorylation of the Na^+,K^+-ATPase [38, 39].

Based on a slow relaxation of the E1/E2 equilibrium, now let us consider the origin of the RH421 fluorescence change. Our analysis of the kinetic data shown in Fig. 4 indicates that prior to the addition of P_i one would expect 58% of the enzyme to be in the E1 conformation and 42% in the E2 conformation. Therefore, if the fluorescence response were due to either phosphate binding to the protein or to phosphorylation itself, one would expect a biphasic fluorescence response. There should be a rapid jump in fluorescence due to the phosphorylation of enzyme initially in E2, followed by a slower increase in fluorescence as enzyme redistributes from E1 to E2 prior to undergoing phosphorylation. Because the enzyme was initially fairly evenly distributed between E1 and E2, the two phases would be expected to have similar amplitudes. However, no such behaviour was observed (see Figs. 1-3). In agreement with previous data obtained using shark rectal gland enzyme [39], the fluorescence response of RH421 to phosphorylation by P_i is monophasic. This indicates that both binding of P_i to the Na^+,K^+-ATPase and phosphorylation itself are fluorescently "silent" reactions for RH421. The entire fluorescence response can be attributed to the E1 → E2 conformational change.

Now that we know that the voltage-sensitive probe RH421 responds to a conformational change of the Na^+,K^+-ATPase, the next question is how a conformational change can produce a change in local electric field strength which the dye can detect. For this purpose we first analysed the expected hydrophobic thickness of the Na^+,K^+-ATPase in different conformational states. The analysis indicated that there are local deformations of lipids around the protein that differ in the $E1P \cdot ADP \cdot 3Na^+$ and $E2 \cdot P_i \cdot 2K^+$ states, approaching 10% of the bilayer thickness on average. It is, thus, possible that membrane deformations may make some contribution towards the RH421 response. The magnitude of the RH421

response and the fact that minimal fluorescence changes are observed when the dye used on the SR Ca^{2+}-ATPase, which one would expect to undergo similar motions of its trans-membrane domains, would seem to suggest, however, that membrane hydrophobic thickness changes are unlikely to be the only or even the major contributor to the RH421 response. Another possibility is that RH421 could be responding to conformational changes of the Na^+,K^+-ATPase by interacting directly with the protein [36, 37]. Prior investigations have shown that RH421 can bind to proteins and some poly(amino acids) [37] and evidence has been presented suggesting that the origin of the interaction is via the dye's hydrophilic sulfonate residue [36, 37], presumably with positively charged basic lysine or arginine amino acid residues of the protein. From trypsin digest experiments it is known that significant movements of the N-terminal sequence of the α-subunit of the Na^+,K^+-ATPase accompany the E2-E1 conformational transition [74-76]. The N-terminus is particularly lysine-rich and has been proposed to act as a movable ion-selective gate during cation binding and occlusion [77]. Therefore, it would appear now that the most likely cause of the RH421 response is an interaction of the protein's N-terminus either with the surface of the surrounding membrane or a penetration of some of the N-terminus a short distance into the membrane (i.e. no deeper than the lipid headgroup region, according to the quantum mechanical calculations of the dye's absorbance spectrum). The latter would be expected to perturb lipid packing and change the membrane dipole potential, to which RH421 is known to be sensitive [9, 10, 85-89].

To test the possibility of N-terminal interaction of the Na^+,K^+-ATPase with its surrounding membrane as a possible cause of the RH421 response, we used poly-L-lysine as a model of the N-terminus. It was found that the addition of poly-L-lysine to Na^+,K^+-ATPase-containing membrane fragments causes changes in the visible absorbance spectrum of the dye which were very similar to those produced by phosphorylation of the protein by ATP. This

supports the idea that the dye is in fact responding to a change in the interaction of the N-terminus with the membrane, and suggests that the N-terminus moves onto to the membrane during the E1 → E2P transition. Quantum mechanical calculations of the dye's absorbance spectrum were also found to be consistent with a neutralisation of the negative charge of the dye's sulfonate group by positive charge, which could arise from lysines of the N-terminus.

The results obtained here suggest that membrane binding and release of the N-terminus of the Na^+,K^+-ATPase play an important mechanistic role in the catalytic cycle of the protein. This further supports recent results suggesting that electrostatic interactions between the protein's N-terminus and the surrounding membrane play a central role in the self-inhibitory regulation of Na^+,K^+-ATPase activity [78].

ACKNOWLEDGEMENT

The authors thank Prof. Simon Ho, University of Sydney, and Assoc. Prof. Stefan Paula, Purdue University, for helpful discussions and Frau Helga Husmann for figure preparation. Financial support was received from the Australian Research Council (Discovery Grants DP-121003548, DP-150101112 and DP-170101732), the National Health and Medical Research Council of Australia (APP1104259) and the National Computational Initiative of Australia (dd7). D. J. acknowledges the European Research Council (ERC) and the Région des Pays de la Loire for financial support in the framework of a Starting Grant (Marches 278845) and the LumoMat project, respectively. This research used resources of (i) the GENCI-CINES/IDRIS, (ii) CCIPL (Centre de Calcul Intensif des Pays de Loire), and (iii) a local Troy cluster.

REFERENCES

[1] W. N. Ross, B. M. Salzberg, L. B. Cohen, A. Grinvald, H. V. Davila, A. S. Waggoner, C. H. Wang, Changes in absorption, fluorescence, dichroism and birefringence in stained giant axons: optical measurement of membrane potential, J. Membr. Biol. 33 (1977) 141-183.

[2] A. S. Waggoner, Dye indicators of membrane potential, Ann. Rev. Biophys. Bioeng. 8 (1979) 47-68.

[3] A. Grinvald, R. D. Frostig, E. Lieke R. Hildesheim, Optical imaging of neuronal activity, Physiol. Rev. 68 (1988) 1285-1366.

[4] L. M. Loew, How to choose a potentiometric membrane probe, in: Spectroscopic Membrane Probes, vol. 2, L. M. Loew (Ed.), CRC Press, Boca Raton, FL, 1988, pp 139-151.

[5] P. Fromherz, K. H. Dambacher, H. Ephardt, A. Lambacher, C. O. Muller, R. Neigl, H. Schaden, O. Schenk, T. Vetter, Fluorescent dyes as probes of voltage transients in neuron membranes: progress report, Ber. Bunsenges. Phys. Chem. 95 (1991) 1333-1345.

[6] M. Zochowski, M. Wachowiak, C. X. Falk, L. B. Cohen, Y. W. Lam, S. Antic, D. Zecevic, Imaging membrane potential with voltage-sensitive dyes, Biol. Bull. 198 (2000) 1-21.

[7] B. Kuhn, P. Fromherz, Annellated hemicyanine dyes in a neuron membrane: molecular Stark effect and optical voltage recording, J. Phys. Chem. B 110 (2003) 13624-13632.

[8] V. V. Shynkar, A. S. Klymchenko, G. Duportail, A. P. Demchenko, Y. Mély, Two-colour fluorescent probes for imaging the dipole potential of cell plasma membranes, Biochim. Biophys. Acta – Biomembr. 1712 (2005) 128-136.

[9] A. P. Demchenko, Y. Mély, G. Duportail, A. S. Klymchenko, Monitoring biophysical properties of lipid membranes by environment-sensitive fluorescent probes, Biophys. J. 96 (2009) 3461-3470.

[10] R. J. Clarke, Electric field sensitive dyes, in: Advanced Fluorescence Reporters in Chemistry and Biology I: Fundamentals and Molecular Design, Springer Series on Fluorescence Vol. 8, A. P. Demchenko (vol. Ed.), O. S. Wolfbeis (series Ed.), Springer, Berlin, 2010, pp 331-344.

[11] W. Liptay, Electrochromism and solvatochromism, Angew. Chem. Int. Ed. Engl. 8 (1969) 177-188.

[12] P. R. Callis, Electrochromism and solvatochromism in fluorescence response of organic dyes: a nanoscopic view, in: Advanced Fluorescence Reporters in Chemistry and Biology I: Fundamentals and Molecular Design, Springer Series on Fluorescence Vol. 8, A. P. Demchenko (vol. Ed.), O. S. Wolfbeis (series Ed.), Springer, Berlin, 2010, pp 309-330.

[13] L. M. Loew, G. W. Bonneville, J. Surow, Charge shift optical probes of membrane potential. Theory, Biochemistry 17 (1978) 4065-4071.

[14] A. Grinvald, R. Hildesheim, VSDI: A new era in functional imaging of cortical dynamics. Nature Rev. Neurosci. 5 (2004) 874-885.

[15] I. Klodos, B. Forbush III, Rapid conformational changes of the Na/K pump revealed by a fluorescent dye, J. Gen. Physiol. 92 (1988) 46a.

[16] J. Heberle, N. A. Dencher, Surface-bound optical probes monitor proton translocation and surface potential changes during the bacteriorhodopsin photocycle, Proc. Natl. Acad. Sci. U. S. A. 89 (1992) 5996-6000.

[17] P. R. Pratap, J. D. Robinson, Rapid kinetic analyses of the Na^+/K^+-ATPase distinguish among different criteria for conformational change, Biochim. Biophys. Acta 1151 (1993) 89-98.
[18] I. Klodos, Partial reactions in Na^+/K^+- and H^+/K-ATPase studied with voltage-sensitive fluorescent dyes, in: The Sodium Pump: Structure Mechanism, Hormonal Control and Its Role in Disease, E. Bamberg and W. Schoner (Eds.), Steinkopff, Darmstadt, Germany, 1994, pp 517-528.
[19] M. Pedersen, M. Roudna, S. Beutner, M. Birmes, B. Reifers, H.-D. Martin, H.-J. Apell, Detection of charge movements in ion pumps by a family of styryl dyes, J. Membr. Biol. 185 (2002) 221-236.
[20] A. Diller, O. Vagin, G. Sachs, H.-J. Apell, Electrogenic partial reactions of the gastric H,K-ATPase, Biophys. J. 88 (2005) 3348-3359.
[21] R. J. Clarke, Probing kinetics of ion pumps via voltage-sensitive fluorescent dyes, in: Fluorescence Applications in Biotechnology and in the Life Sciences, E. M. Goldys (Ed.), Wiley-Blackwell, Hoboken, NJ, 2009, pp 349-363.
[22] A. Pilotelle-Bunner, F. Cornelius, P. Sebban, P. W. Kuchel, R. J. Clarke, Mechanism of Mg^{2+} binding in the Na^+,K^+-ATPase, Biophys. J. 96 (2009) 3753-3761.
[23] M. Khalid, F. Cornelius, R. J. Clarke, Dual mechanisms of allosteric acceleration of the Na^+,K^+-ATPase by ATP, Biophys. J. 98 (2010) 2290-2298.
[24] S. L. Myers, F. Cornelius, H.-J. Apell, R. J. Clarke, Kinetics of K^+ occlusion by the phosphoenzyme of the Na^+,K^+-ATPase, Biophys. J. 100 (2011) 70-79.
[25] Grădinaru, R. V., and H.-J. Apell, Probing the extracellular access channel of the Na,K-ATPase, Biochemistry 54 (2015) 2508-2519.
[26] D. W. Hilgemann, Channel-like function of the Na,K pump probed at microsecond resolution in giant membrane patches, Science 263 (1994) 1429-1432.
[27] C.-C. Lu, A. Kabakov, V. S. Markin, S. Mager, G. A. Frazier, D. W. Hilgemann, Membrane transport mechanisms probed by capacitance measurements with megahertz voltage clamp, Proc. Natl. Acad. Sci. U. S. A. 92 (1995) 11220-11224.
[28] R. F. Rakowski, D. C. Gadsby, P. De Weer, Voltage dependence of the Na/K pump, J. Membr. Biol. 155 (1997) 105-112.
[29] D. C. Gadsby, F. Bezanilla, R. F. Rakowski, P. De Weer, M. Holmgren, The dynamic relationships between the three events that release individual Na^+ ions from the Na^+/K^+-ATPase, Nature Commun. 3 (2012) 669.
[30] J. P. Castillo, H. Rui, D. Basilio, A. Das, B. Roux, R. Latorre, F. Bezanilla, M. Holmgren, Mechanism of potassium ion uptake by the Na^+/K^+-ATPase, Nature Commun. 6 (2015) 7622.
[31] L. J. Mares, A. Garcia, H. H. Rasmussen, F. Cornelius, Y. A. Mahmmoud, J. R. Berlin, B. Lev, T. W. Allen, R. J. Clarke, Identification of electric-field-dependent steps in the Na^+,K^+-pump cycle, Biophys. J. 107 (2014) 1352-1363.
[32] R. D. Peluffo, Y. Hara, J. R. Berlin, Quaternary organic amines inhibit Na,K pump in a voltage-dependent manner: direct evidence of an extracellular access channel in the Na,K-ATPase, J. Gen. Physiol. 123 (2004) 249-263.
[33] R. D. Peluffo, R. M. González-Lebrero, S. B. Kaufman, S. Kortagere, B. Orban, R. C. Rossi, J. R. Berlin, Quaternary benzyltriethylammonium ion binding to the Na,K-ATPase: A tool to investigate extracellular K^+ binding reactions, Biochemistry 48 (2009) 8105-8119.
[34] R. D. Peluffo, J. R. Berlin, Membrane potential-dependent inhibition of the Na^+,K^+-ATPase by para-nitrobenzyltriethylammonium bromide, Mol. Pharmacol. 82 (2012) 1-8.

[35] R. J. Clarke, Dipole-potential-mediated effects on ion pump kinetics, Biophys. J. 109 (2015) 1513-1520.
[36] N. U. Fedosova, F. Cornelius, I. Klodos, Fluorescent styryl dyes as probes for Na,K-ATPase reaction mechanism: Significance of the charge of the hydrophilic moiety of RH dyes, Biochemistry 34 (1995) 16806-16814.
[37] J. Frank, A. Zouni, A. van Hoek, A. J. W. G. Visser, R. J. Clarke, Interaction of the fluorescent probe RH421 with ribulose-1,5-bisphosphate carboxylase/oxygenase and with Na^+,K^+-ATPase membrane fragments, Biochim. Biophys. Acta – Biomembr. 1280 (1996) 51-64.
[38] H.-J. Apell, M. Roudna, J. E. T. Corrie, D. R. Trentham, Kinetics of the phosphorylation of Na,K-ATPase by inorganic phosphate detected by a fluorescence method, Biochemistry 35 (1996) 10922-10930.
[39] F. Cornelius, N. U. Fedosova, I. Klodos, E2P phosphoforms of Na,K-ATPase. II. Interaction of substrate and cation-binding sites in P_i phosphorylation of Na,K-ATPase, Biochemistry 37 (1998) 16686-16696.
[40] J. C. Skou, M. Esmann, Preparation of membrane Na^+,K^+-ATPase from rectal glands of *Squalus acanthias*, Methods Enzymol. 156 (1988) 43-46.
[41] I. Klodos, M. Esmann, R. L. Post, Large-scale preparation of sodium-potassium ATPase from kidney outer medulla, Kidney Int. 62 (2002) 2097-2100.
[42] P. R. Pratap, O. Dediu, G. U. Nienhaus, FTIR study of ATP-induced changes in Na^+/K^+-ATPase from duck supraorbital glands, Biophys. J. 85 (2003) 3707-3717.
[43] P. Ottolenghi, The reversible delipidation of a solubilized sodium-potassium ion-dependent adenosine triphosphatase, Biochem. J. 151 (1975) 61-66.
[44] U. Banik, S. Roy, A continuous fluorometric assay for ATPase activity, Biochem. J. 266 (1990) 611-614.
[45] P. R. Pratap, E. H. Hellen, A. Palit, J. D. Robinson, Transient kinetics of substrate binding to Na^+/K^+-ATPase measured by fluorescence quenching, Biophys. Chem. 69 (1997) 137-151.
[46] G. L. Peterson, A simplification of the protein assay method of Lowry et al. which is more generally applicable, Anal. Biochem. 83 (1977) 346-356.
[47] O. H. Lowry, N. J. Rosebrough, A. L. Farr, R. J. Randall, Protein measurement with the Folin phenol reagent, J. Biol. Chem. 193 (1951) 265-275.
[48] A. Zouni, R. J. Clarke, A. J. W. G. Visser, N. V. Visser, J. F. Holzwarth, Static and dynamic studies of the potential-sensitive membrane probe RH421 in dimyristoylphosphatidylcholine vesicles, Biochim. Biophys. Acta – Biomembr. 1153 (1993) 203-212.
[49] A. Zouni, R. J. Clarke, J. F. Holzwarth, Kinetics of solubilisation of styryl dye aggregates by lipid vesicles, J. Phys. Chem. 98 (1994) 1732-1738.
[50] F. Cornelius, Functional reconstitution of the sodium pump. Kinetics of exchange reactions performed by reconstituted Na/K-ATPase, Biochim. Biophys. Acta 1071 (1991) 19-66.
[51] S. Amoroso, V. V. Agon, T. Starke-Peterkovic, M. D. McLeod, H.-J. Apell, P. Sebban, R. J. Clarke, Photochemical behaviour and Na^+,K^+-ATPase sensitivity of voltage-sensitive styrylpyridinium fluorescent membrane probes, Photochem. Photobiol. 82 (2006) 495-502.
[52] T. H. N. Pham, R. J. Clarke, Solvent dependence of the photochemistry of the styrylpyridinium dye RH421, J. Phys. Chem. B 112 (2008) 6513-6520.
[53] M. J. Frisch, G. W. Trucks, H. B. Schlegel, G. E. Scuseria, M. A. Robb, J. R. Cheeseman, G. Scalmani, V. Barone, B. Mennucci, G. A. Petersson, H. Nakatsuji, M. Caricato, X. Li, H. P. Hratchian, A. F. Izmaylov, J. Bloino, G. Zheng, J. L.

Sonnenberg, M. Hada, M. Ehara, K. Toyota, R. Fukuda, J. Hasegawa, M. Ishida, T. Nakajima, Y. Honda, O. Kitao, H. Nakai, T. Vreven, J. A. Montgomery, Jr., J. E. Peralta, F. Ogliaro, M. Bearpark, J. J. Heyd, E. Brothers, K. N. Kudin, V. N. Staroverov, R. Kobayashi, J. Normand, K. Raghavachari, A. Rendell, J. C. Burant, S. S. Iyengar, J. Tomasi, M. Cossi, N. Rega, J. M. Millam, M. Klene, J. E. Knox, J. B. Cross, V. Bakken, C. Adamo, J. Jaramillo, R. Gomperts, R. E. Stratmann, O. Yazyev, A. J. Austin, R. Cammi, C. Pomelli, J. W. Ochterski, R. L. Martin, K. Morokuma, V. G. Zakrzewski, G. A. Voth, P. Salvador, J. J. Dannenberg, S. Dapprich, A. D. Daniels, Ö. Farkas, J. B. Foresman, J. V. Ortiz, J. Cioslowski, and D. J. Fox, Gaussian 09, Revision D.01, Gaussian, Inc., Wallingford CT, 2009.

[54] Y. Zhao, D. G. Truhlar, The M06 suite of density functionals for main group thermochemistry, thermochemical kinetics, noncovalent interactions, excited states, and transition elements: two new functionals and systematic testing of four M06-class functionals and 12 other functionals, Theor. Chem. Acc. 120 (2008) 215-241.

[55] A. V. Marenich, C. J. Cramer, D. G. Truhlar, Universal solvation model based on solute electron density and a continuum model of the solvent defined by the bulk dielectric constant and atomic surface tensions, J. Phys. Chem. B 113 (2009) 6378-6396.

[56] R. J. Clarke, A. Zouni, J. F. Holzwarth, Voltage sensitivity of the fluorescent probe RH421 in a model membrane system, Biophys. J. 68 (1995) 1406-1415.

[57] R. Kanai, H. Ogawa, B. Vilsen, F. Cornelius, C. Toyoshima, Crystal structure of a Na^+-bound Na^+,K^+-ATPase preceding the E1P state, Nature 502 (2013) 201-206.

[58] J. P. Morth, B. P. Pedersen, M. S. Toustrup-Jensen, T. L.-M. Sørensen, J. Petersen, J. P. Andersen, B. Vilsen, P. Nissen, Crystal structure of the sodium-potassium pump, Nature 450 (2007) 1043-1049.

[59] S. Jo, T. Kim, V. G. Iyer, W. Im, Software news and updates – CHARM-GUI: A web-based graphical user interface for CHARMM, J. Comput. Chem. 29 (2008) 1859-1865.

[60] J. C. Phillips, R. Braun, W. Wang, J. Gumbart, E. Tajkhorshid, E. Villa, C. Chipot, R. D. Skeel, L. Kale, K. Schulten, Scalable molecular dynamics with NAMD, J. Comput. Chem. 26 (2005) 1781-1802.

[61] A. D. MacKerell, M. Feig, C. L. Brooks, Extending the treatment of backbone energetics in protein force fields: Limitations of gas-phase quantum mechanics in reproducing protein conformational distributions in molecular dynamics simulations, J. Comput. Chem. 25 (2004) 1400-1415.

[62] J. B. Klauda, R. M. Venable, J. A. Freitas, J. W. O'Connor, D. J. Tobias, C. Mondragon-Ramirez, I. Vorobyov, A. D. MacKerell, R. W. Pastor, Update of the CHARMM all-atom additive force field for lipids: Validation on six lipid types, J. Phys. Chem. B 114 (2010) 7830-7843.

[63] S. E. Feller, Y. H. Zhang, R. W. Pastor, Computer-simulation of liquid/liquid interfaces. 2. Surface-tension area dependence of a bilayer and monolayer, J. Chem. Phys. 103 (1995) 10267-10276.

[64] J.-P. Ryckaert, G. Ciccotti, H. J. Berendsen, Integration of the Cartesian equations of motion of a system with constraints: Molecular dynamics simulation of *n*-alkanes, J. Comput. Phys. 23 (1977) 327-341.

[65] U. Essmann, L. Perera, M. L. Berkowitz, T. Darden, H. Lee, L. G. Pedersen, A smooth particle mesh Ewald method, J. Chem. Phys. 103 (1995) 8577-8593.

[66] B. A. Lewis, D. M. Engelman, Lipid bilayer thickness varies linearly with acyl chain length in fluid phosphatidylcholine vesicles, J. Mol. Biol. 166 (1983) 211-217.

[67] M. A. Lomize, A. L. Lomize, I. D. Pogozheva, H. I. Mosberg, OPM: Orientations of proteins in membranes database, Bioinformatics 22 (2006) 623-625.
[68] M. Nyblom, M., H. Poulsen, P. Gourdon, L. Reinhard, M. Andersson, E. Lindahl, N. Fedosova, and P. Nissen, Crystal structure of Na^+,K^+-ATPase in the Na^+-bound state, Science 342 (2013) 123-127.
[69] T. Shinoda, T., H. Ogawa, F. Cornelius, C. Toyoshima, Crystal structure of the sodium-potassium pump at 2.4 Å resolution, Nature 459 (2009) 446-450.
[70] A. Witzke, K. Lindner, K. Munson, H.-J. Apell, Inhibition of the gastric H,K-ATPase by clotrimazole, Biochemistry 49 (2010) 4524-4532.
[71] C. Butscher, M. Roudna, H.-J. Apell, Electrogenic partial reactions of the SR-Ca-ATPase investigated by a fluorescence method, J. Membr. Biol. 168 (1999) 169-181.
[72] C. Peinelt, H.-J. Apell, Kinetics of Ca^{2+} binding to the SR Ca-ATPase in the E1 state, Biophys. J. 89 (2005) 2427-2433.
[73] A. Fibich, H.-J. Apell, Kinetics of luminal proton binding to the SR Ca-ATPase, Biophys. J. 101 (2011) 1896-1904.
[74] P. L. Jørgensen, E. Skriver, H. Hebert, A. B. Maunsbach, Structure of the Na,K pump: Crystallization of pure membrane-bound Na,K-ATPase and identification of functional domains of the α-subunit, Ann. N. Y. Acad. Sci. 402 (1982) 207-225.
[75] P. L. Jørgensen, J. H. Collins, Tryptic and chymotryptic cleavage sites in sequence of alpha-subunit of (Na^+ + K^+)-ATPase from outer medulla of mammalian kidney, Biochim. Biophys. Acta 860 (1986) 570-576.
[76] P. L. Jørgensen, J. P. Andersen, Structural basis for E1-E2 conformational transitions in Na,K-pump and Ca-pump proteins, J. Membr. Biol. 103 (1988) 95-120.
[77] G. E. Shull, J. Greeb, J. B. Lingrel, Molecular cloning of three distinct forms of the Na^+,K^+-ATPase α-subunit from rat brain, Biochemistry 25 (1986) 8125-8132.
[78] Q. Jiang, A. Garcia, M. Han, F. Cornelius, H.-J. Apell, H. Khandelia, R. J. Clarke, Electrostatic stabilization plays a central role in autoinhibitory regulation of the Na^+,K^+-ATPase, Biophys. J., in press (accepted 6th December, 2016).
[79] K. P. Wheeler, R. Whittam, The involvement of phosphatidylserine in adenosine triphosphatase activity of the sodium pump, J. Physiol. 207 (1970) 303-328.
[80] F. Cornelius, M. Habeck, R. Kanai, C. Toyoshima, and S. J. D. Karlish, General and specific lipid-protein interactions in Na,K-ATPase, Biochim. Biophys. Acta – Biomembr. 1848 (2015) 1729-1743.
[81] D. Volodkin, H. Mohwald, J.-C. Voegel, V. Ball, Coating of negatively charged liposomes by polylysine: Drug release study, J. Controlled Release 117 (2007) 111-120.
[82] A. Hädicke, A. Blume, Binding of the cationic peptide $(KL)_4K$ to lipid monolayers at the air-water interface: Effect of lipid headgroup charge, acyl chain length, and acyl chain saturation, J. Phys. Chem. B 120 (2016) 3880-3887.
[83] S. Kumar, G. Stecher, K. Tamura, MEGA7: Molecular evolutionary genetics analysis version 7.0 for bigger datasets, Mol. Biol. Evol. 33 (2016) 1870-1874.
[84] B. Le Guennic, D. Jacquemin, Taking up the cyanine challenge with theoretical tools, Acc. Chem. Res. 48 (2015) 530-537.
[85] E. Gross, R. S. Bedlack Jr., L. M. Loew, Dual-wavelength ratiometric fluorescence measurement of the membrane dipole potential, Biophys. J. 67 (1994) 208-216.
[86] R. J. Clarke, D. J. Kane, Optical detection of membrane dipole potential: avoidance of fluidity and dye-induced effects, Biochim. Biophys. Acta – Biomembr. 1323 (1997) 223-239.

[87] J. Cladera, P. O'Shea, Intramembrane molecular dipoles affect the membrane insertion and folding of a model amphiphilic peptide, Biophys. J. 74 (1998) 2434-2442.
[88] R. J. Clarke, The dipole potential of phospholipid membranes and methods for its detection, Adv. Colloid Interfac. Sci. 89-90 (2001) 263-281.
[89] A. P. Demchenko, S. O. Yesylevskyy, Nanoscopic description of biomembrane electrostatics: results of molecular dynamics simulations and fluorescence probing, Chem. Phys. Lipids 160 (2009) 63-84.